2017 IEEE International Conference on Advanced Intelligent Mechatronics (AIM)
Sheraton Arabella Park Hotel, Munich, Germany, July 3-7, 2017

Design, Fabrication, and Dynamics of an Electromagnetic Vertical Microactuator for Endomicroscopy*

Jiawei Zhang, Clark B. Teeple, Jongsoo Choi, Samantha Kang, Joseph E. Rivas, and Kenn R. Oldham, *Member, IEEE*

Abstract— **Advanced microscopy techniques can permit imaging beneath the tissue surface in hollow organs where cancer can begin. This work examines the design, modeling, fabrication and control process for an electromagnetic z-displacement, or into-tissue, scanning microactuator based on semiconductor fabrication methods. Dynamic modeling and control of the microactuator allows it to perform large vertical displacements despite nonlinearities of thick-film magnetic material behavior and closely-spaced dynamic modes from the compliant actuator structures. Nearly single frequency oscillation of >100 µm vertical displacement at 15 V is achieved by implementing an open-loop input linearization control tsignal. Nearly pure vertical motion of the microstage prevents the focal point of actuator lens from deviating from an axial laser path, necessary to capture images with high resolution.**

I. Introduction

Conventional white light endomicroscopy for cancer detection in the gastrointestinal system has a high polyp miss rate due to difficulty in detecting flat lesions. Novel microscopy techniques, such as dual axes confocal [1] [2] and multi-photon [3] [4] microscopy can provide sufficient penetration depth and resolution to perform rapid optical sectioning and vertical cross-sectional images below the tissue surface. In combination with molecular biomarkers, these techniques could dramatically improve cancer detection and monitoring. However, to effectively image cross-sections of tissue in real-time by these methods, it is necessary to have fast vertical scanning actuators that can be implemented in form factors compatible with endoscopic use.

In recent years, many microelectromechanical system (MEMS) scanning mirrors have been proposed for laser scanning in small endomicroscopic instruments. In particular, deep tissue imaging requires axial scanning of laser light along the direction of a laser. Microactuators with large axial deflection, or vertical motion from the silicon chip surface on which their mirror surfaces are built, have previously been demonstrated using various transduction methods, including electrostatic, electrothermal, and piezoelectric actuation [5] [6] [7] [8] [9]. Large displacement, in this context, indicates a vertical translation that is a substantial percentage (often 10-20%) of the maximum dimension of the chip, on the order of 100 µm or greater. Relative to these approaches, electromagnetic transduction is potentially attractive for eliminating a need for direct electrical connections to the MEMS chip, as motion can be induced through electromagnetic coupling from a coil in the endomicroscope housing. For purposes of confocal microscopy, Siu et al. have previously used this principle to demonstrate vertical scanning of a PDMS micro-lens on magnetic nickel platform and compliant spring, achieving vertical displacement of 125 µm with a resonant frequency of 215 Hz [10].

This paper presents a monolithic permalloy microactuator for high-speed vertical scanning in an endomicroscope form factor, in which the complete stage structure is fabricated from a single electroplated permalloy layer. Actuators formed from a single permalloy layer have advantages for both simplifying actuator processing and assembly and providing excellent actuator mechanical robustness compared to other thin-film vertical actuators. Stages were successfully fabricated using semiconductor micro-fabrication techniques to prepare a silicon wafer followed by permalloy deposition after characterizion of electroplating parameters to obtain favorable material composition (20% iron, 80% nickel.

The resulting monolithic microactuator architecture gives rise to several closely-spaced elastic vibration modes, which in interaction with nonlinear magnetic response can give rise to complex dynamic responses that substantially influence actuator performance. The dynamic modeling of permalloy-based microactuators has received relatively limited prior attention. While the magnetization of magnetic thin-films has heavily studied for sensing and data storage applications, microactuator dynamics have generally been examined in quasi-static [11] [12] or linear dynamic regimes [10] [13]. To explain additional phenomena observed with the microactuators described here, it is found to be necessary to examine the effects of magnetic nonlinearity on multiple modes in the elastic actuator structure. A basic two degree of freedom system is used to model the primary dynamic modes of the magnetic stage. Magnetic forcing is implemented using

*Research supported by National Science Foundation, award CMMI 1334340 and the National Institutes for Health, award R01EB020644.

J. Zhang is with the University of Michigan Department of Mechanical Engineering, Ann Arbor, MI.

C.B. Teeple was with the University of Michigan Department of Mechanical Engineering. He is now with Harvard University, Cambridge, MA.

J. Choi was with the University of Michigan Department of Mechanical Engineering. He is now with Vesper Technologies, Boston, MA.

S. Kang was with the University of Washington Department of Mechanical Engineering. She is now with Hewlett Packard, Inc.

J. Rivas is with Binghampton University Department of Mechanical Engineering, Binghampton, NY.

K.R. Oldham are with the University of Michigan Department of Mechanical Engineering, Ann Arbor, MI 48105 (e-mail: oldham@umich.edu).

a hysteresis model based on prior works on thin-film permalloy magnetization behavior. Higher-order modes and a simple LR model for the electromagnet are then added in series. An ad-hoc feedforward controller inspired by input linearization techniques is designed to obtain a specified sinusoidal displacement for the stage output. Shaped voltage inputs from the feedforward controller improve actuator vertical displacement from less than 20 µm to over 100 µm near resonance, though some modeled sensitivities to input parameters remain to be explained.

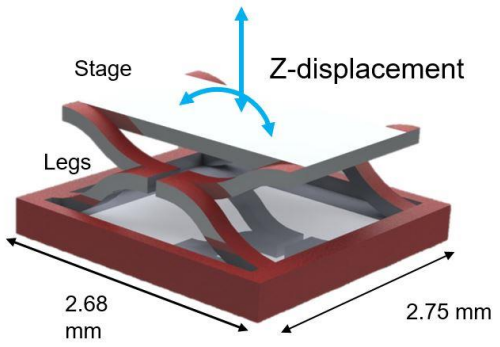

Figure 1. Conceptual architecture of the electromagnetic vertical microactuator.

II. Design

The prototype actuator consists of a central platform with four flexible legs, all coated with electroplated permalloy, that is designed to fit within the center of a dual axes confocal endomicroscope. A magnetic field is applied to the stage in its vertical or z-axis, with the resulting magnetic force acting on the central platform drives the actuator into vertical displacement, though magnetic torques may also be induced by residual off-axis magnetization of the permalloy thin-film. This z-displacement scanning actuators would allow imaging below a tissue surface by moving the focal point of a laser reflected off the mirror surface.

During prototype actuator fabrication, leg and platform geometry were selected based on prior thin-film piezoelectric actuators developed for dual axes confocal endomicroscopy [14]. Outer frame dimensions of 3 mm x 3.2 mm are based on a maximum endomicroscope diameter of 5.5 mm, inner mirror platform dimensions are based on requirements for dog-bone style mirrors used in dual axes axes microscopy, at 2.4 mm x 1.1 mm for the current form factor, and serpentine spring legs were extended over remaining space at the four corners of the stage.

Actuators were manufactured through electroplating of permalloy (Ni/Fe) on a silicon wafer, and patterning compliant beams and a central stage, as shown in Fig. 2. In use as a micro mirror, a high-quality mirror surface would be attached to the central stage. To begin fabrication, seed layers (50Å of chrome (Cr) and 500Å of copper (Cu), respectively) were deposited onto a silicon (Si) wafer using electron beam evaporation. AZ-9260 photoresist was then spin-coated and patterned onto the wafer, and then inserted into a nickel-iron electroplating bath.

The goal of electroplating optimization was to electroplate a thick film (8-10 µm) of permalloy having low residual stress, since excess deformation in the actuators could interfere with its performance. After several characterization tests, we employed a pulse-reverse plating program with an anodic (forward) current density of 20 mA/cm^2 for 20 milliseconds (ms), a cathodic (reverse) current density of -8 mA/cm^2 for 2 ms, and an off time of 10 ms (Fig. 3), as inspired by [15]. After 120 minutes of electroplating, approximately 8 µm of low residual stress permalloy was deposited onto the actuators. Energy dispersive x-ray spectroscopy analysis revealed the permalloy was 88.25% nickel, 11.75% iron, and magnetic. After etching the seed layers, the wafer was processed with xenon difluoride to isotropically etch the Si and release the devices. A sample stage is shown in Fig. 4.

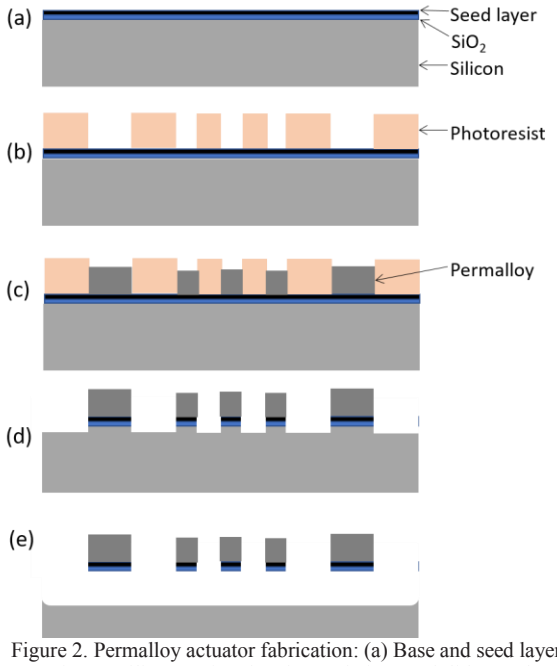

Figure 2. Permalloy actuator fabrication: (a) Base and seed layer preparation on silicon wafer; (b) Electroplating mask lithography; (c) Permalloy electroplating (d) Photoresist removal and seed layer etch; (e) Isotropic XeF_2 release.

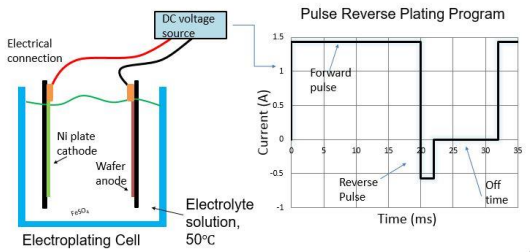

Figure 3. Electroplating set-up and program with reverse pulse to adjust permalloy composition.

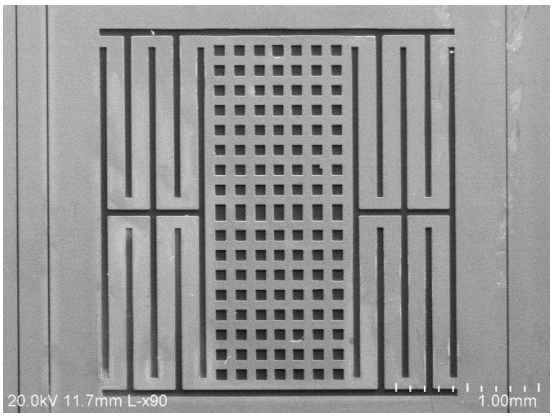

Figure 4. Scanning electron microscope image of electroplated permalloy microactuator

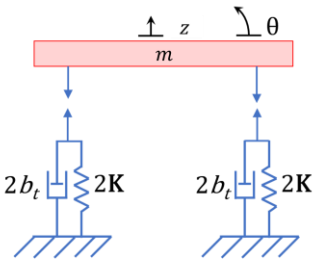

Figure 5. Schematic lumped parameter model for first dynamic modes in *x*-*z* axis.

III. Dynamic Model

Nominal dynamics of the completed stages may be approximated as those of a rigid mass on symmetric multi-axis springs, with equivalent lumped parameter model shown in Fig. 5. Motion is analyzed in the *x*-*z* plane, based on experimental testing showing significant rotation about the *x*-axis in addition to desired z-axis translation, though conceptually analysis can be extended to additional axes, as has been done for piezoelectric microactuator dynamics with similar geometry [14].

For small angular rotations, the first primary modes of deformation can be modeled as dynamically independent, due to symmetry in the low-stress permalloy structure. Each serpentine leg acts as a multi-axis spring with stiffness matrix **K**, which can be reduced to effective vertical stiffness, k_t, and effective rotational stiffness, k_r, based on the elements of **K** and the distance of the legs from the center of the central platform. Then, vertical displacement of the center of the stage relative to rest, z, is given by:

$$m\ddot{z} + b_t\dot{z} + k_t z = F \tag{1}$$

where m is the mass of the platform plus effective mass of the legs, b_t represents translational viscous damping, and F is the magnetic force on the system in the vertical direction.

The angular displacement of the platform, θ, is given by:

$$J\ddot{\theta} + b_r\dot{\theta} + k_r\theta = T \tag{2}$$

where J is the rotational inertia, b_r represents rotational viscous damping, and T is the magnetic torque acting on the stage.

Magnetic force and torque are determined by the strength of the magnetic field and the magnetization of the permalloy film, which as a soft magnetic material also changes with the applied field. While the magnetic force acts as a vector, with orientation affected by the magnetic field, only the vertical component of magnetization and magnetic force are modeled here. The magnetic field in the experimental setup is generated by a solenoid coil placed beneath the actuator. The field is assumed to be directed in the z-direction with magnetic flux density, B_{mag}, estimated from [16] as

$$B_{mag} = \frac{N}{\frac{L_{core}}{\kappa\mu_0} + \frac{L_{gap}}{\mu_0}} i_{LR} \tag{3}$$

where N is the number of winds of wire in the magnet, I_{LR} is the current in the coil, L_{core} is the length of the magnetic core, κ is the relative permeability of the core, L_{gap} is the gap distance between the stage and the electromagnet, and μ0 is the permeability of free space. This approximation is taken to be accurate for electromechanical devices where the gap distance from the coil to the magnetic particle is relatively small (less than the diameter of the core).

Dynamically, the electromagnet is assumed to be a linear LR system with the inductor and resistor in series, so the transfer function from input voltage, Vin, to magnet current, ILR, is given by

$$\frac{I_{LR}}{V_{in}} = \frac{1}{Ls+R} \tag{4}$$

where L is the inductance, and R is the resistance of the electromagnet, and s represents complex frequency.

Magnetization, M, of permalloy film in the vertical direction was modeled as a simple hysteretic function calculated incrementally in time, t, as a function of applied field. The hysteresis approximation used was

$$M(t+\delta t) \approx M_b + \begin{cases} max\left(a_1(i_{LR}-h) + a_3(i_{LR}-h)^3, M(t) + \beta\frac{di_{LR}}{dt}\right), & i_{LR}(t+\delta t) > i_{LR}(t) \\ min\left(a_1(i_{LR}+h) + a_3(i_{LR}+h)^3, M(t) + \beta\frac{di_{LR}}{dt}\right), & i_{LR}(t+\delta t) > i_{LR}(t) \end{cases} \tag{5}$$

where M_b is a small bias to magnetization direction inferred from experimental results, and a_1, a_3, β, and h are parameters selected to approximate the small field hysteresis shape of permalloy film tested in [11]. Vertical force on the stage was then estimated as

$$F(t) = gB_{mag}(t)M(t) \tag{6}$$

where g is a constant gain estimated from the volume, shape and permeability of the actuator.

Combined dynamics of the system are shown schematically in Fig. 6, where $G_{LR}(s)$ is the linear dynamics of the coil from (4), f_1 represents the nonlinear magnetization model, $G_1(s)$ is the linear dynamic model for the first two modes. Linear system $G_2(s)$ is used to describe any additional higher-order modes relevant to the frequency range of interest, identified experimentally.

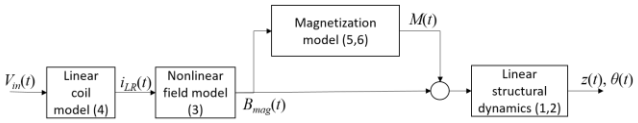

Figure 6. Components of electromagnetic actuator model.

IV. Controller Design

The goal of controller design is to ensure that a large and sinusoidal displacement (i.e. pure z-axis translation near the z-axis resonance) is achieved in the presence of electromagnetic nonlinearities that excite higher-order modes of the actuator structure when driven by a raw sinusoidal input. In effect, an input signal is to be designed such that the force, F_{in}, is a close as possible to a pure sinusoid, by inverting the magnetic nonlinearity. While many more rigorous hysteresis inversion techniques are known, for example for sinusoidal tracking with a Preisach model [17], in the current work an *ad hoc* approach is taken. To approximate a desired in input force, $F_d(t) = A \sin \omega t$, where ω is a desired operating frequency and A is a constant to be maximized given a nominal voltage limit, a desired flux density, B_d, is generated from

$$B_d(t) = \sqrt{|A \sin \omega t|} \cdot \text{sign}(A \sin \omega t). \quad (7)$$

This alteration of the input signal acts to slow the rate of change of the magnetic field during the portion of a cycle that magnetization is changing rapidly, and speed up the change of the magnetic field when magnetization is relatively insensitive to field, thus restoring the output of (6) to a forcing that more closely approximates a pure sine.

To implement the input shaping in (7), inversion of the remaining components of the model is performed first into a desired current, i_d, then to a desired voltage, V_d,

$$i_d(t) = \frac{B_d(t)}{N}\left(\frac{L_{core}}{\kappa\mu_0} + \frac{L_{gap}}{\mu_0}\right) \quad (8)$$

$$V_d(s) = \frac{10^6(Ls+R)}{(s+1000)(s+1000)} I_d(s) \quad (9)$$

where poles in (9) are selected to be much faster than the target operating frequency. Given a maximum permissible input voltage for a given coil, V_{max}, the shaped input is optimized by maximizing A from (7) subject to $\max(V_d(t) < V_{max})$.

V. Results

A. Parameter Identification

Experimental testing was performed using a modified solenoid coil in a three-axis micropositioner to permit adjustment of the magnetic field. Stage velocity/displacement at multiple points was monitored using a Laser Doppler Vibrometer (LDV) and X-Z sensor with custom input signals generated by LabVIEW.

Various model parameters were identified experimentally. These include inductance and resistance of the electromagnet, as well as its magnetic field, as the number of turns in the solenoid coil was not known. Relative thickness of the permalloy film in the central platform and legs was also tuned to account for variation in deposition rate with feature size by matching the frequency ratio between the first two vibration modes (z translation versus x rotation). Similarly, damping coefficients were estimated from the half-power width of the resonant peaks. Finally, the apparent magnetization strength of the permalloy film was estimated based on the small-signal displacement of the actuator given the relatively well-characterized mass, stiffness, and magnetic field.

The resulting mechanical model shows good agreement with experimentally-observed small-signal or single-sided motion, as shown in Fig. 2, when magnetic nonlinearities do not produce frequency doubling effects. Upper curves in Fig 2 show the frequency response for tilt of the stage, while the lower set of curves show the translational response. While vertical translation is the focus of the current work, throughout the current set of experiments tilt angles were on approximately 0.5º near the first z-axis resonance, driven by components of the magnetization vector not in the vertical axis; this response was also in close agreement with modeled behavior after gain and damping identification, with first resonance for tilt around 670 Hz, versus 600-625 Hz for vertical translation.

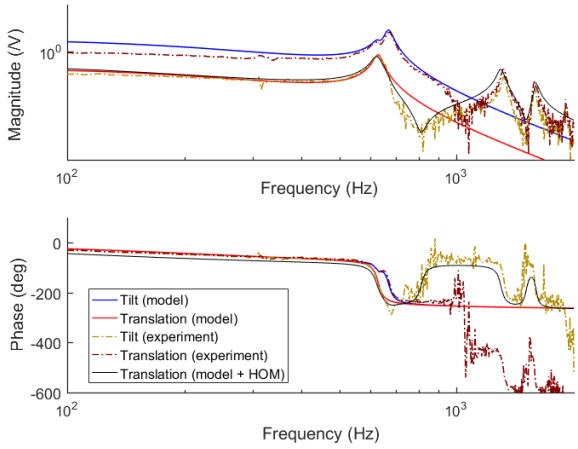

Fig. 7. Simulated and experimental small signal output amplitude and phase versus input frequency; It should be noted that for large field excitation, frequency doubling of the input occurs due to magnetic nonlinearity, such that mechanical resonance near 600 Hz is excited by an input at 300 Hz.

B. Vertical Scanning

Fig. 8 shows modest vertical displacement of the permalloy actuator under a pure sinusoidal input at 300 Hz, which would nominally excite resonant motion at 600 Hz due to the effect of the square of magnetic field on the magnetic force. Although not obvious in the displacement profile (Fig. 8, bottom), higher order modes near 1200 and 1700 Hz excited by harmonics of the input signal after hysteresis effects have significant impact on amplitude. This is clearer in the direct LDV velocity output (Fig. 8, top), which significantly

deviates from a pure sinusoidal output and shows harmonic oscillations above the main oscillation frequency of 600 Hz. The resulting displacement, about 17 µm peak-to-peak, is

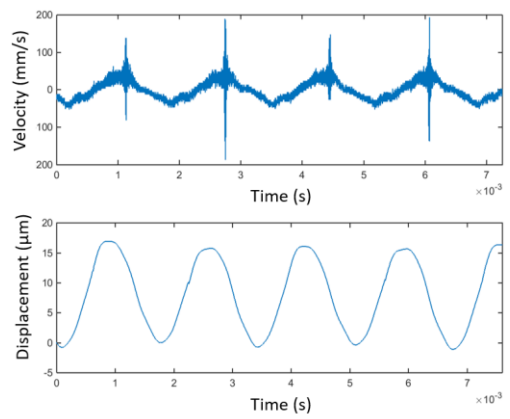

Fig.8. Actuator response to sinusoidal input at 300 Hz, measured by LDV, shows substantial deviation from a sinusoidal output in velocity response (top) due to excitation of higher-order modes, and resulting limited vertical translations of about 17 µm peak-to-peak (bottom)

much smaller than would be expected from the analytical model for the vertical displacement mode alone.

Figure 9 shows the shaped input applied to mitigate hysteresis effects, and Fig. 10 shows the resulting displacement profile. Output displacement from the actuator is increased over five-fold, to nearly 115 µm, with almost pure sinusoidal output concentrated at twice the actuation frequency, as shown in Fig. 11.

This behavior is successfully predicted by the actuator model, as shown in Fig. 12, though in practice the improvement with input shaping is even more dramatic than anticipated by the model. Model-based predictions for amplitude with sinusoidal and shaped inputs are approximately 25 µm and 102 µm, respectively. Experimental sine response being worse and shaped response being better than predicted is likely due to incomplete knowledge about the permalloy hysteresis behavior, though it is also possible that additional filtering effects may be present in inductor or instrumentation dynamics.

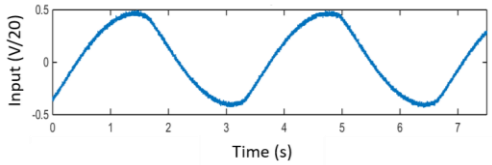

Fig. 9. Shaped input applied to the permalloy actuator at 300 Hz.

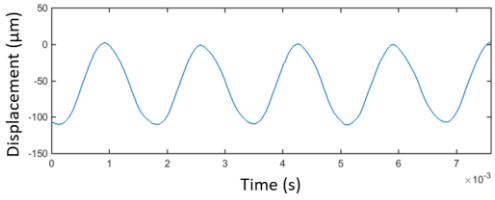

Fig. 10. With shaped input for approximate magnetic nonlinearity cancellation, periodic displacement exceeds 110 µm.

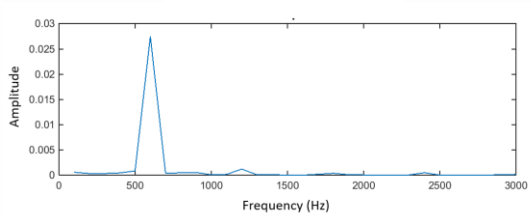

Fig. 11. Nearly pure sine response using shaped input is confirmed from FFT analysis of the displacement response data shown in Fig. 10.

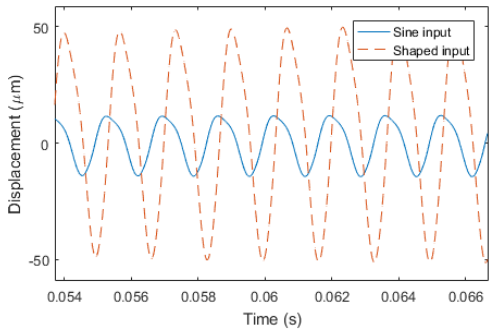

Fig. 12. Simulated steady-state response of the permalloy actuator correctly anticipates large improvement in displacement amplitude using shaped input, though improvement is about 10% less than observed experimentally, with more deviation from pure sinusoidal output.

VI. Discussion and Conclusions

Experimental and simulated actuator displacements shown in Section V illustrate the substantial effects that nonlinear magnetic forcing can have on elastic structures susceptible to motion from significant higher-order modes. Ideally, this can be addressed from the design of the actuators, to avoid having higher order modes close to integer multiples of the intended primary resonance, as occurs in the prototype devices. However, process control during permalloy electroplating is imprecise, and it is often necessary instead to rely on controller design to mitigate unintended dynamic effects. This work shows that a simple re-shaping of the control input can potentially return actuator response to a nearly sinusoidal response, though naturally more sophisticated hysteresis inversion and/or feedback control techniques are available.

As a technology for vertical cross-sectional imaging in endomicroscopy instruments, the current actuators provide a moderate range of total vertical displacement, up to about 115 µm under a 15 V input signal from a 10 mm diameter solenoid coil, with an operating resonance of 600 Hz. This is a smaller stroke but higher bandwidth than most prior vertical actuators for endomicroscopy, which have achieved 200-400 µm displacement with first structural resonance in the range of 100-200 Hz (i.e. works [7-10]). Exceptions include electrostatic micormirrors, which have achieved comparable or higher stroke and operating frequency but at much larger voltages, typically on the order of 60-100 V (see, for example, [4]). In addition, it must be noted that adding a micro-mirror would be expected to decrease resonance frequency by 10-25%, and in smaller instruments, a smaller coil size would be required with associated larger voltages and current needs.

Given the current performance and performance limitations, the primary benefits of this actuator architecture are to simplify assembly of an endomicroscopic imaging probe and to improve structural robustness. An electromagnetic coil for wireless excitation of a scanning mirror is often much simpler to install and align in a small diameter instrument than electrical connections directly to a MEMS chip, and 10-15 μm thick metal alloy elastic elements are substantially mechanically stronger than the bending elements most prior thin-film vertical microactuators. This work also verifies the potential for good control of permalloy composition based on adjustment to electroplating waveforms.

From a dynamics and analysis perspective, this work provides a very basic framework for modeling behaviors in permalloy actuators. The simple input shaping function that is proposed dramatically improves actuator range of motion for the prototype actuators. However, there remains substantial validation and refinement of these dynamic model components to be done in future work. Without direct measurement of permalloy magnetization, the hysteresis model is derived from previously reported permalloy magnetization loop shapes and inferred behavior in the current system, which we would expect this to be an imperfect match to the true magnetization response of the deposited permalloy film. Likewise, the feedforward input chosen in this work, while effective, is not fully justified from a modeling standpoint. In future work, we will examine methods for more rigorous identification of hysteresis properties from dynamic actuator response across a range of frequencies and voltages, and use that to improve assessment of the current and alternative hysteresis inversion techniques.

ACKNOWLEDGMENT

The authors thank Dr. Pilar Herrera-Fierro and the staff of the Lurie Nanofabrication Facility for help in development of the electromagnetic actuators, and the National Science Foundation National Nanotechnology Infrastructure Network Research Experience for Undergraduates program for their support of Ms. Samantha Kang and Mr. Joseph E. Rivas.

REFERENCES

[1] J. Liu, M. Mandella, H. Ra, L. Wong, O. Solgaard, G. Kino, W. Piyawattanmetha, C. Congag and T. Wang, "Miniature near-infrared dual-axes confocal microscope utilizing a two-dimensional microelectromechanical scanner," *Optics Letters,* vol. 32, no. 3, pp. 256-258, 2007.

[2] Z. Qiu, S. Khondee, X. Duan, H. Li, M. Mandella, B. Joshi, Q. Zhou, S. Owens, K. Kurabayashi, K. Oldham and T. Wang, "Vertical cross-sectional imaging of colonic dysplasia in vivo with multi-spectral dual axes confocal endomicroscopy," *Gastroenterology,* vol. 146, no. 3, pp. 615-617, 2014.

[3] L. Fu, A. Jain, H. Xie, C. Cranfield and M. Gu, "Nonlinear optical endoscopy based on a double-clad photonic crystal fiber and a MEMS mirror," *Optics Express,* vol. 14, no. 3, pp. 1027-1032, 2006.

[4] X. Duan, H. Li, Z. Qiu, B. Joshi, A. Pant, A. Smith, K. Kurabayashi, K. Oldham and T. Wang, "MEMS-based multiphoton endomicroscope for reptitive imaging of mouse colon," *Biomedical Optics Express,* vol. 6, no. 8, pp. 3074-3083, 2015.

[5] C. Ataman, H. Urey and A. Wolter, "A fourier transform spectrometer using resonant vertical comb actuators," *Journal of Micromechanics and Microengineering,* vol. 16, p. 2517, 2006.

[6] A. Jain and H. Xie, "Electrothermal microlens scanner with low-voltage large displacement actuation," *IEEE Photonics Technology Letters,* vol. 17, no. 9, pp. 1971-1973, 2005.

[7] K. Jia, S. Pal and H. Xie, "An electrothermal tip-tilt-piston micromirror based on folded dual s-shaped bimorphs," *Journal of Microelectromechanical Systems,* vol. 18, no. 5, pp. 1004-1015, 2009.

[8] Z. Qiu, J. Pulskamp, X. Lin, C.-H. Rhee, T. Wang, R. Polcawich and K. Oldham, "Large displacement vertical translational actuator based on piezoelectric thin films," *Journal of Micromechanics and Microengineering,* vol. 20, no. 7, p. 075016, 2010.

[9] W. Liao, Y. Zhu, W. Liu, L. Liu, Y. Tang, B. Wang and H. Xie, "A tip-tilt-piston micromirror with symmetrical lateral-shift-free microactuators," *IEEE Sensors Journal,* vol. 13, no. 8, pp. 2873-2881, 2013.

[10] C. Siu, H. Zeng and M. Chiao, "Magnetically actuated MEMS microlens scanner for in vivo medical imaging," *Optics Express,* vol. 15, no. 18, pp. 11154-11166, 2007.

[11] C. Pan and S. Shen, "Electromagnetically actuated bi-direction microactuators with permmaloy and Fe/Pt hard magnet," *Journal of Magnetism and Magnetic Materials,* vol. 285, pp. 422-432, 2005.

[12] C. Liu, T. Tsao, G.-B. Lee, J. Leu, Y. Yi, Y.-C. Tai and C. Ho, "Out-of-plane magnetic actuators with electroplated permalloy for fluid dynamics control," *Sensors and Actuators A: Physical,* vol. 78, no. 2-3, pp. 190-197, 1999.

[13] S. Isikman, O. Egerneman, A. Yalcinkaya and H. Urey, "Modeling and characterization of soft magnetic film actuated 2-D scanners," *IEEE Journal of Selected Topics in Quantum Electronics,* vol. 12, no. 2, p. 283, 2007.

[14] J. Choi, Z. Qiu, C.-H. Rhee, T. Wang and K. Oldham, "A three-degree-of-freedom thin-film PZT actuated microactuator with large out-of-plane displacement," *Journal of Micremechanics and Microengineering,* vol. 24, p. 075017, 2014.

[15] D. Flynn and M. Desmulliez, "Influence of pulse reverse plating on the properties of Ni-Fe thin films," *IEEE Transactions on Magnetics,* vol. 46, no. 4, pp. 979-985`, 2010.

[16] R. Feynman, Lectures on Physics, vol. 2, New York: Addison-Wesley, 1963.

[17] M. Kozek and B. Gross, "Identification and inversion of magnetic hysteresis for sinusoidal magnetization," *International Journal on Online Engineering,* vol. 1, no. 1, 2005.